1-13-2021

MIT-S1 Constitutive Model Calibration for a Portland-area Soil

Steven Ryan Young
Portland State University

MIT-S1 Constitutive Model Calibration for a Portland-area Soil

by

Steven Ryan Young

A thesis submitted in partial fulfillment of
the requirements for the degree of

Master of Science
in
Civil and Environmental Engineering

Thesis Committee:
Diane Moug
Arash Khosravifar
Peter Dusicka

Portland State University
2020

Abstract

Soils that are intermediate to sands and clays are a challenge for geotechnical engineers since most methods for interpreting soil properties or soil behaviors are based on sands or clays and do not address behaviors of intermediate soils. This is a particular challenge for engineers in the Portland-area where many of the major soil units are composed of intermediate soils. Analysis of intermediate soils is further challenged since many standard constitutive models are based on sandy or clay-like soils. However, the MIT-S1 constitutive model is capable of capturing intermediate soil behavior. A calibration of the MIT-S1 constitutive model for Portland-area intermediate soils is presented. Calibration of an MIT-S1 constitutive model for a Portland-area intermediate soil will be useful for developing relationships with in-situ tests such as the cone penetration test (CPT). The calibration includes a limited compression curve (LCC) characterization of a silt slurry mixture sourced from a local soil unit to establish high stress, 1-D compression parameter values. Numerical analysis is included for additional key constitutive model properties. Parameter values are derived through the use of the model simulation software (Itasca FLAC) and comparison to laboratory data from undrained direct simple shear (UDSS) tests. The calibration prioritizes MIT-S1 model parameters associated with 1-D compression and the transition from contractive to dilative behavior in shear.

Table of Contents

Table of Figures - Section 2

Table of Figures - Section 3

1. Introduction

Geotechnical site characterization is a critical step for the design of building and infrastructure projects. Site characterization generally consists of one or more different methods including soil sampling, lab testing of soil specimen, and in-situ testing. In-situ testing is particularly useful for characterization by providing information on local soil properties with minimal disturbance. The cone penetration test, or CPT, is a common method of in-situ analysis. The CPT provides a nearly continuous data profile of the subsurface conditions based on cone tip resistance, skin friction and pore water pressure. These data can be analyzed and interpreted to help estimate the engineering and soil properties for the site.

CPT interpretation is well understood for drained penetration in sands and undrained penetration in clays (Moug et al 2019). However, for soils intermediate to sands and clays ("intermediate soils"), there is a large uncertainty regarding how to interpret engineering properties from CPT data, in particular those properties that effect liquefaction triggering analysis such as fines content (Boulanger and Idriss 2016). This is a particular problem in the Portland area where many major soil units are intermediate soils, such as Columbia River alluvium deposits or Willamette silt (also known as Missoula Flood deposits).

The research documented in this paper is a part of a larger study to develop region-specific CPT interpretations for the Portland-area. This includes how liquefaction susceptibility relates to CPT measurements. Currently, determining whether silts have the potential to liquefy due to ground motions during an earthquake requires costly and time-consuming lab work. One potential outcome of this larger project will allow practicing engineers to make determinations about liquefaction potential at project sites with simple, in-situ explorations and tests such as the cone penetration test (CPT). One aspect of the research is to perform an investigation of soil behavior around the CPT, and how CPT data relate to engineering properties, with a numerical cone penetration model and soil model calibrated for Portland-area soils.

The goal of this project is to develop a calibration for the MIT-S1 constitutive model that approximates soil behavior for Columbia River alluvium. The MIT-S1 constitutive model is capable of capturing the stress-strain-strength properties of soils from sands to clays, including intermediate soils. MIT-S1 is a bounding surface elasto-plastic constitutive model. In-depth descriptions of the model are available in Pestana and Whittle (1999), Pestana et al. (2002) Additionally, a description of MIT-S1 as implemented in FLAC is provided in Jaeger (2012). The calibration will be implemented with a direct cone penetration model in the finite difference program FLAC (Moug et al. 2019) for future research.

2. High Stress 1-D Compression Testing

A primary feature of the MIT-S1 constitutive model is the limiting compression curve (LCC) (Figure 2.1). The LCC describes soil compression behavior at high stresses and is linear in a log-log void ratio, *e* - effective stress space. The mechanism of volumetric change in the LCC regime is soil dependent. For sands or sand-like soils, LCC characterization is independent of initial relative density, as the primary volumetric change in the LCC regime is caused by particle crushing. Under very high stress loading in 1-D compression, soil specimens of the same type will fall along the same curve, regardless of initial relative density. The slope of the curve is identified in the MIT-S1 model as ρ_c. The intersection of the slope at a void ratio of 1.0 is identified as the reference vertical stress, $\sigma_{v,ref}$. Characterization of the LCC is necessary to establish key parameters for the MIT-S1 constitutive model.

2.1 Lab Testing Procedures

LCC characterization for this study was accomplished by performing high stress (up to 150MPa) 1-D compression tests. The 1-D compression testing was done using a pneumatic load frame with a maximum load capacity of approximately 1100kN (250kip) which was donated to PSU from AECOM (Figures 2.2, 2.3, and 2.4). Measurement of applied force was observed with an analogue load gauge installed on the load frame and data was captured with an in-line load cell installed in the hydraulic line of the load frame. The load cell is capable of measuring load increments as small as 1.33kN (300lbf), approximately. Deflection of the specimen is measured by movement of the upper platen with an LVDT secured to the immobile lower platen of the load frame with a magnetic clamp. Captured data is recorded to a computer using Measurement & Automation Explorer v4.7 from National Instruments.

A mold and piston apparatus was designed and constructed using 4140 tool-grade quenched and tempered steel (ACRALLOY) for use with the load frame described above (Figures 2.5 and 2.6). The design of the mold and piston was a modified version of the vessel and cap used by Parra Bastidas (2016). The specimen mold was designed to be 2.5-in. diameter and 1.5-in. deep. This allows for soil specimen volumes and dimensions that are typical for oedometer and direct simple shear tests. The piston fits within the mold opening with a gap tolerance of 0.002-in. This small tolerance value allows the piston to deflect vertically under load while minimizing the effects of rocking, bridging, and differential stress.

The piston was designed to be 2-in tall with two grooves cut around the perimeter of the cylinder in the lower third of the device for the installation of o-rings. The o-rings ensure a proper seal between the walls of the mold and the piston in order to direct water from a saturated sample in 1-D compression to the drainage holes. The height of the piston was intended to be taller than the mold depth to better facilitate removal in the case of the piston being inserted without a specimen. Small (0.125-in. diameter) drainage holes were drilled in both the mold and the piston for control of drained 1-D compression tests. Cylindrical cavities were routed into the mold and piston surface over the drainage holes so that porous stones could be inserted. A 0.25-in threaded hole was tapped through the top of the piston so that a bolt could be inserted and used to assist extraction of the piston.

For general 1-D compression testing, the piston is prepared by installing o-rings and applying a light coating of silicon lubricant to the o-rings. The lubricant helps to reduce issues with friction and facilitated smoother movement of the piston during the compression test. The piston is then placed in the mold and carefully seated on to the specimen. The piston is checked with a small torpedo level to ensure it is seated flat. The height of the piston over the lip of the mold is measured with a set of digital calipers in a minimum of three locations around the perimeter and the measurements are arithmetically averaged. This averaged measurement is recorded for data processing steps to determine initial volume of the specimen.

Following the specimen preparation, the mold is placed on the lower platen of the load frame. To avoid eccentric loading conditions, the mold is centered relative to the upper platen and verified through visual inspection. The upper platen is lowered until it just reaches the point of contact with the top of the piston.

Data capture for the 1-D compression test is done using the VI Logger program included in the Measurement & Automation Explorer software package. This software captures voltage readings from the load cell and LVDT which is then transformed to respective force and length measurements calibrated against known measurement devices. Calibration of the load cell was done by comparison to an analog force gauge built into the load frame which was in turn calibrated with a 100kip (445kN) load cell. The LVDT was calibrated using an acrylic block of known thickness. Load frame system calibrations were performed with the assistance of Tom Bennett.

With the mold and piston in place, the 1-D compression test is performed by engaging the load frame. The load frame is controlled manually with a four-position lever (Retract, Off, Metered Advanced, Full Advance) (Figure 2.4). The speed of the metered advance position can be adjusted with a valve installed in-line with the hydraulic feed. For this study, the adjustment valve is set for the slowest movement speed possible. This allows the software to best capture the small deflection increments necessary to characterize the initial LCC curve transition. The load is increased until the analogue gauge indicates an applied load of 45 kips (150MPa) at which point the lever was set to the off position for approximately 5 seconds before reversal and unloading.

The data captured during 1-D compression is then processed for LCC characterization. Physical measurement of specimen volume and mass was used to determine the initial specimen void ratio, e_0

$$e_0 = \frac{V_v}{V_s} \tag{2.1}$$

where V_v is volume of voids and V_s is volume of solids and

$$V_v = V - V_s \tag{2.2}$$

where

$$V_s = \frac{m}{G_s} \tag{2.3}$$

$$V = \frac{h\pi d^2}{4} \tag{2.4}$$

where V is total specimen volume, m is mass, G_s is the specific gravity of soil particles, and h and d are the height and diameter of the specimen, respectively.

2.2 Testing on Ottawa F-65 Sand

Initial 1-D compression tests were conducted on Ottawa F-65 sand ("Ottawa sand") for the purpose of validating the test procedures. Ottawa sand is a uniform quartzite sand with well-understood and studied material properties (Parra Bastidas 2016). Ottawa sand specimens were prepared using the following method. An appropriate quantity of the specimen material was selected by visual inspection, weighed, and placed in the mold. Specimen placement was done by dry pluviation. This consisted of funneling the sand into the mold in a roughly circular pattern around the mold from a height just above the top edge of the vessel. For these tests, specimens were prepared "dense" by lightly tapping and/or agitating the mold following pluviation. The agitation also served to level the specimen prior to placing the piston.

Deflection data captured via LVDT during 1-D compression was used to determine changes to e during compression and loading force data was used to determine stress. Void ratio was plotted against stress in a double logarithmic space. MIT-S1 constitutive model parameters ρ_c, θ, and $\sigma'_{v,ref}$ were determined from the resulting plot. The slope of the LCC in the double-logarithmic e – σ'_v space in the MIT-S1 model is represented by ρ_c and $\sigma'_{v,ref}$ is the reference vertical stress at e = 1.0 (Figure 2.7).

Results of LCC characterization from 1-D compression lab tests of Ottawa sand using the methods described in Section 2.1 showed a ρ_c value of 0.47, which is similar to the results published in Parra Bastidas (2016) and Pestana and Whittle

(1995) where ρ_c was found to be 0.48 and 0.45, respectively. A comparison plot of 1-D compression data and LCC from Pestana & Whittle (1995) and Parra Bastidas (2016) is shown in Figure 2.8. Differences in the slope of the LCC between the published studies and the 1-D compression test results achieved here are minimal and appear to be within an acceptable range of experimental variation. The position of the LCC with respect to the reference stress ($\sigma'_{v,ref}$) is very similar to the published results from Pestana & Whittle (1995) but is somewhat lower than what was found by Parra Bastidas (2016). The discrepancy is not pronounced, however, and is likely due to variation in sample characteristics. General agreement with the slope and position of the LCC estimated from 1-D compression tests with those from previous research indicated that the LCC characterization methods discussed above were valid and the methodology could be reasonably applied to the Portland-area soil specimens of interest to the broader study.

2.3 Figures

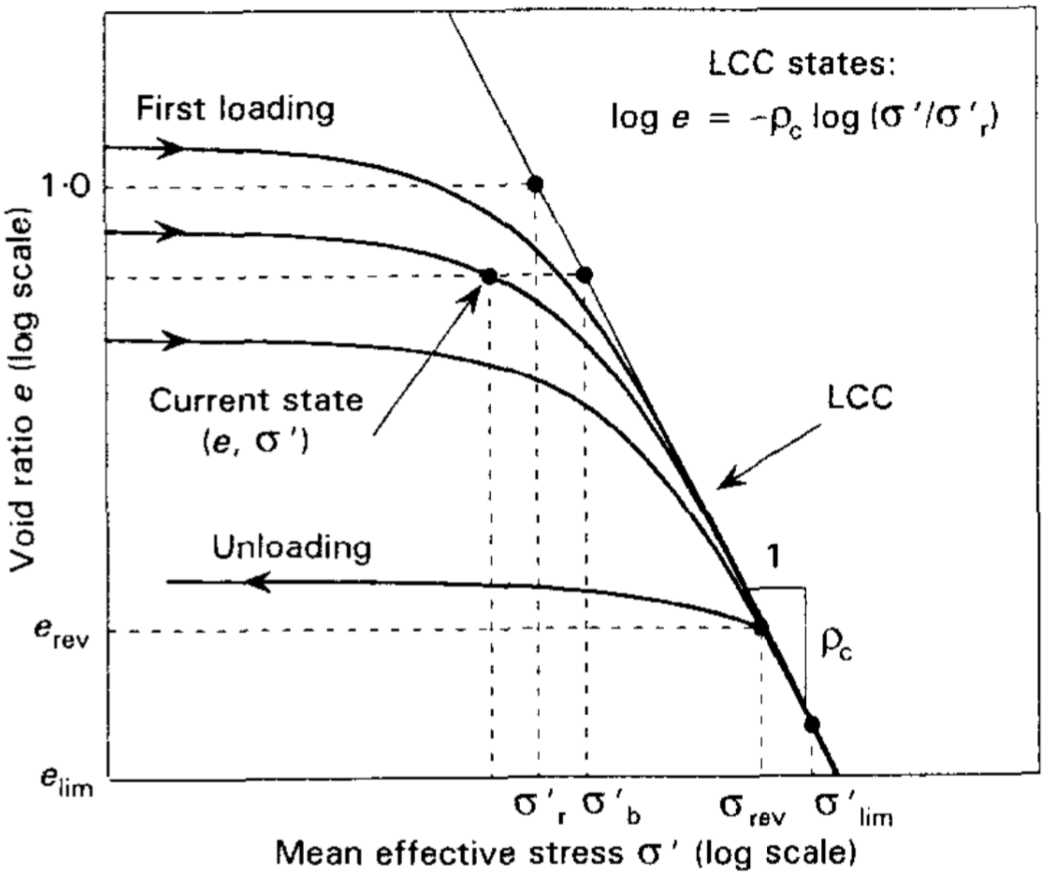

Figure 2.1: Generalized 1-D compression plot showing LCC characterization (reproduced from Pestana & Whittle 1995)

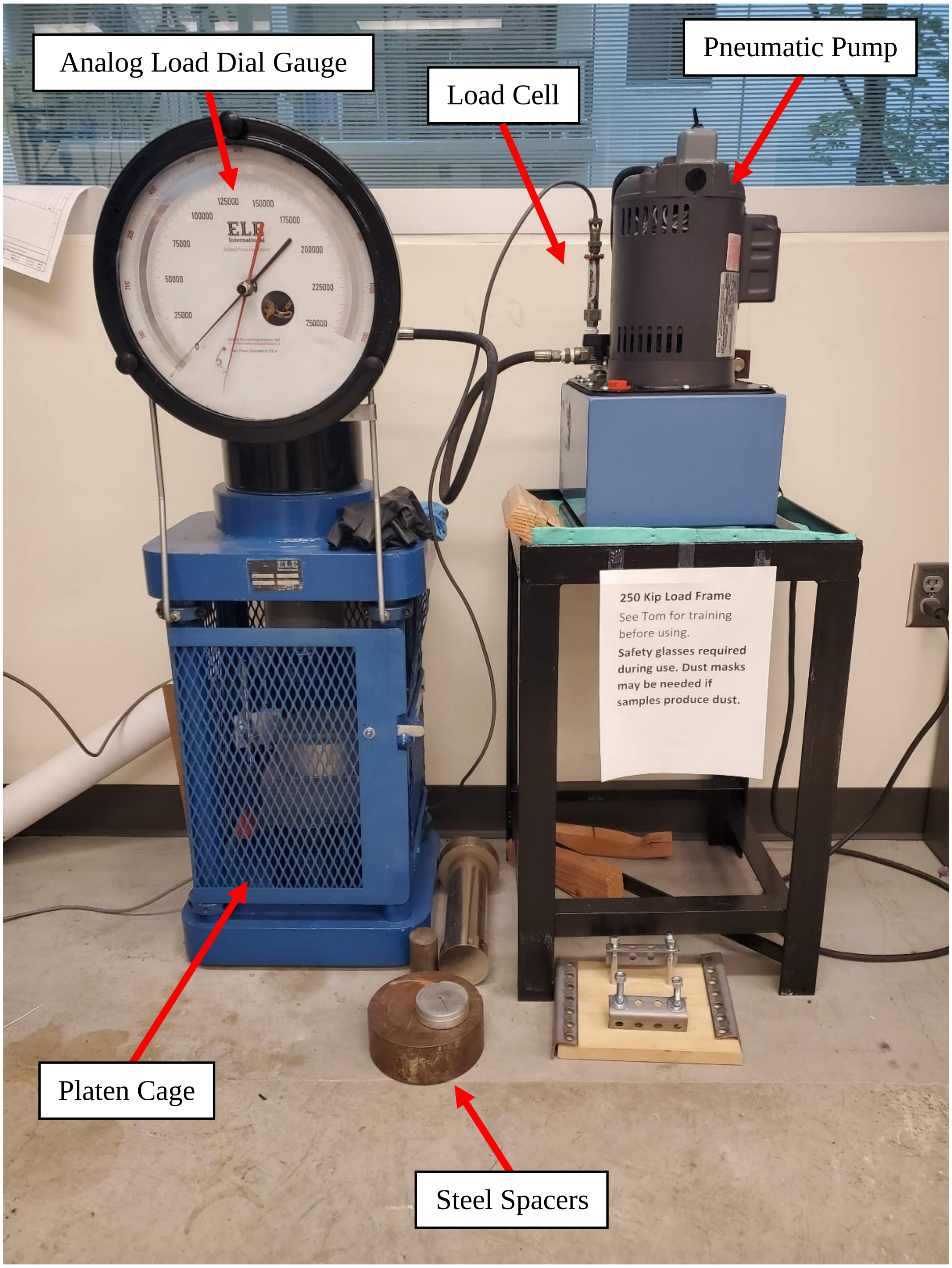

Figure 2.2: Pneumatic load frame used in 1-D compression testing

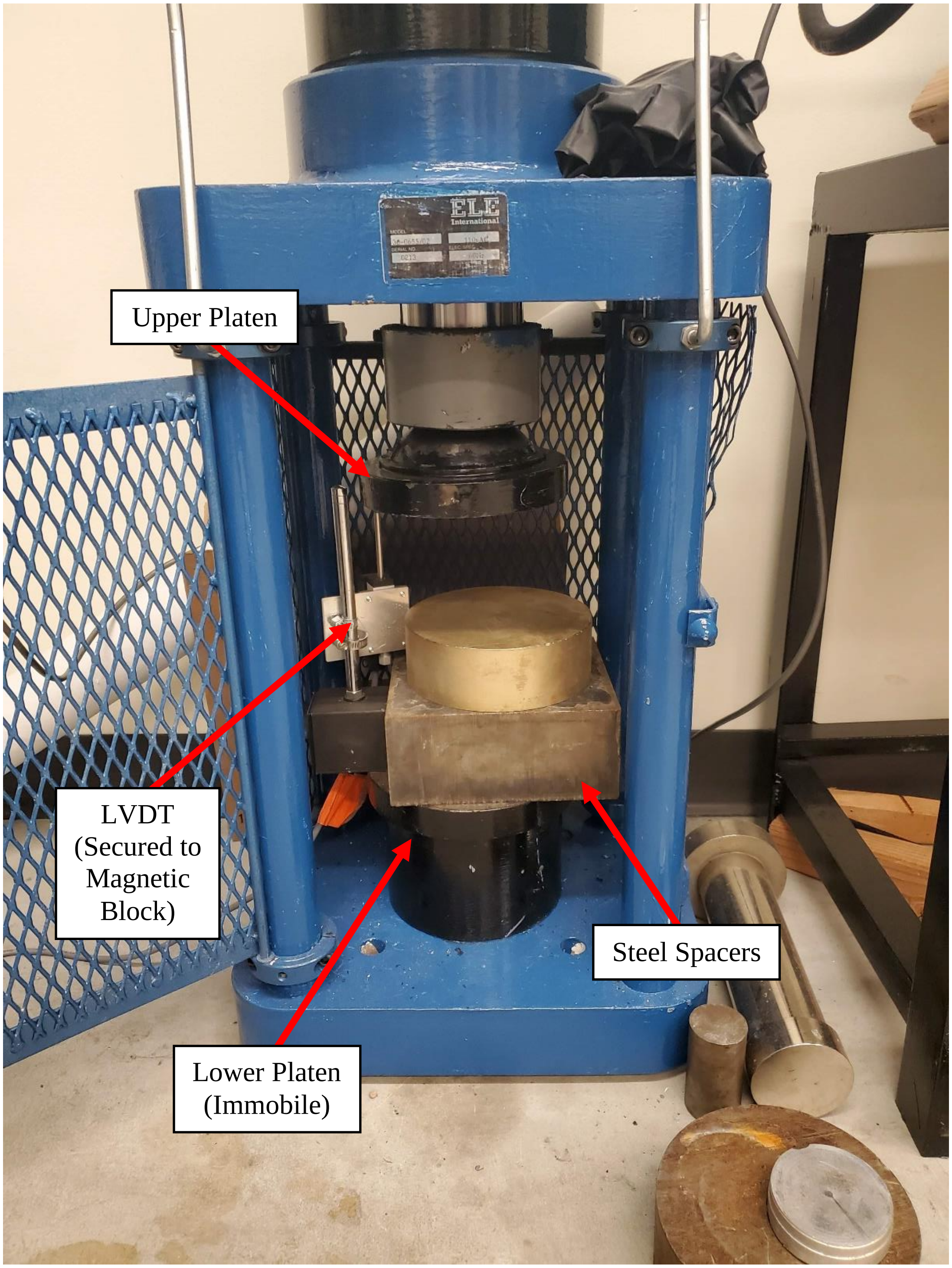

Figure 2.3: Detail of LVDT placement on pneumatic load frame platen

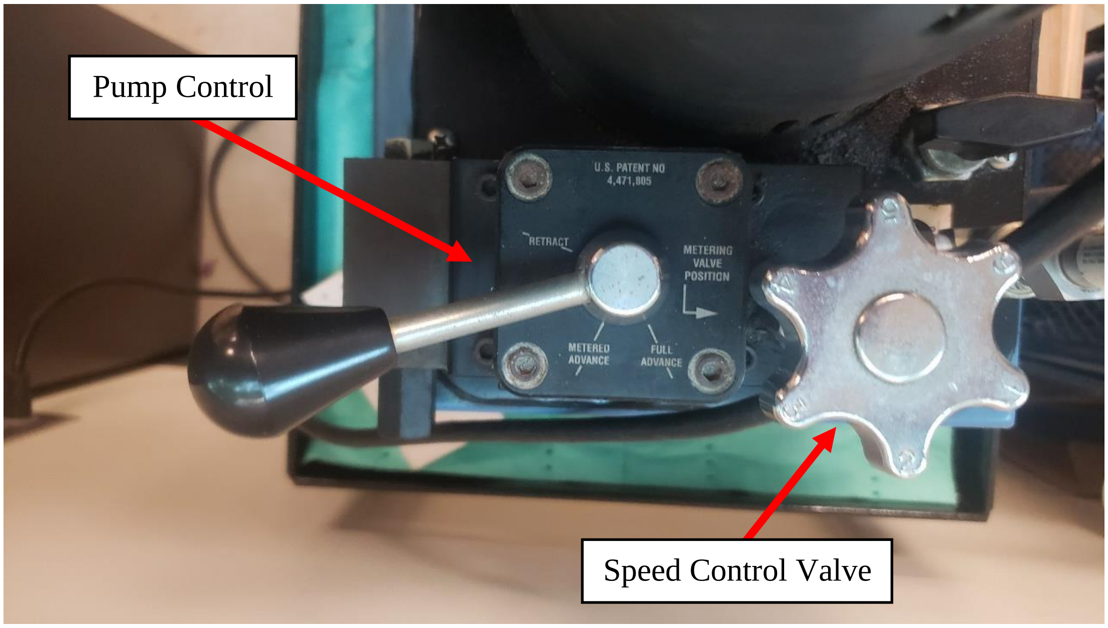

Figure 2.4: Detail of pneumatic pump controls

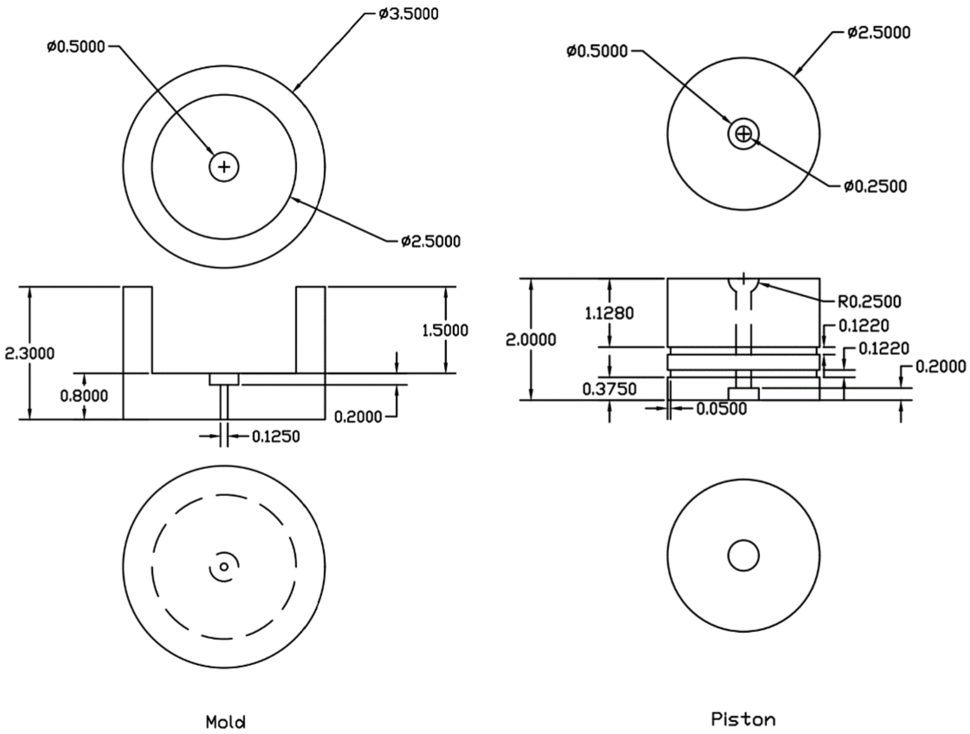

Figure 2.5: Schematic drawing of specimen mold and piston for use in 1-D compression testing

Figure 2.6: Steel (4140 ACRALLOY tool-grade, quenched and tempered) mold and piston device used for 1-D compression testing of soil specimens, seated.

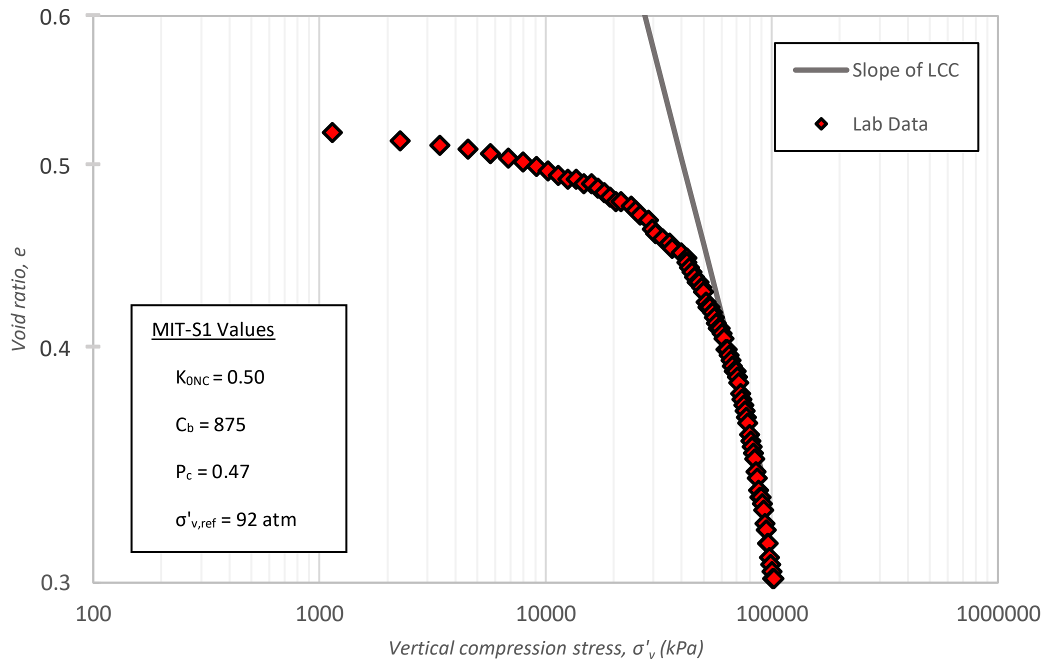

Figure 2.7: 1-D compression plot for Ottawa sand in LCC regime

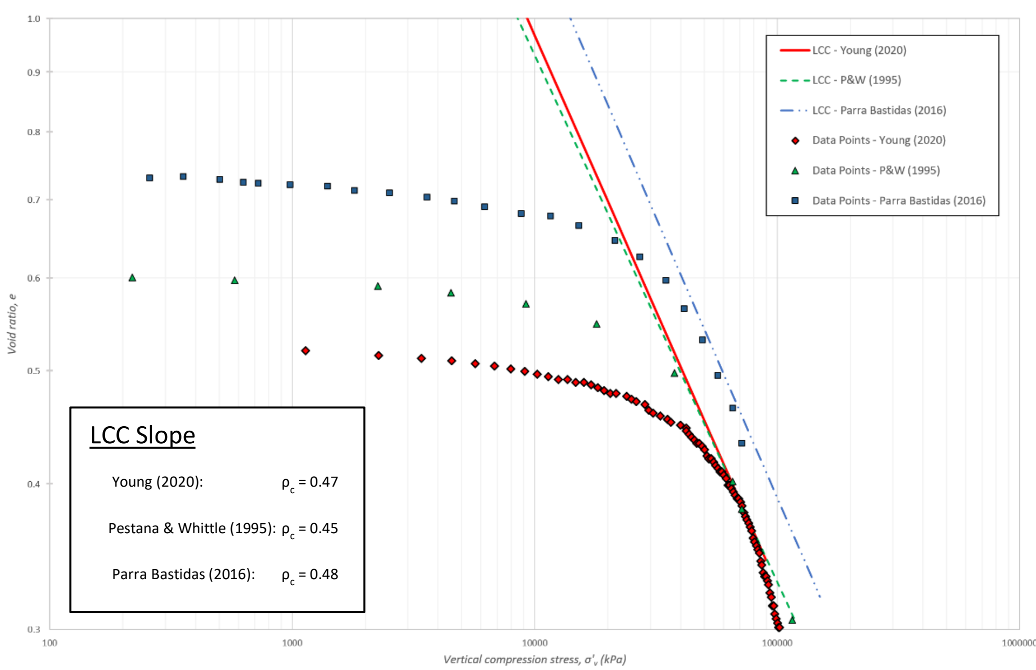

Figure 2.8: 1-D compression plot comparison for Ottawa sand in LCC regime including Pestana & Whittle (1995) and Parra Bastidas (2016) results

3. MIT-S1 Calibration of Columbia River Silt

Calibration of MIT-S1 for a Portland-area silt was done using lab data from undrained direct simple shear tests and 1-D compression tests. The soil sample used to prepare test specimens was sourced from a test site located near the Portland International Airport designated as "Sunderland" (Figure 3.1). The soil samples used for this calibration were collected with Shelby tubes at a depth of approximately 5 meters. The soil was classified as a low-plasticity ML type silt with a plasticity index (PI) of 15, as determined by laboratory visual classification and Atterberg limit tests performed by Kayla Sorenson and Melissa Preciado (Sorenson et al 2021, Preciado et al 2021). Table 3.1 shows general soil properties from the Sunderland research site (Preciado et al 2021). In-situ investigation of the test site was performed with CPT.

Numerical modeling of the constitutive behavior of the soils in this study was conducted with single element simulations with FLAC 8.1. FLAC is an acronym which stands for Fast Lagrangian Analysis of Continua and is a numerical analysis tool designed by Itasca Consulting Group. FLAC uses an explicit finite difference framework to analyze complex behaviors in soils. FLAC was chosen for numerical modeling because of its ability to implement user defined constitutive models and its use in previous research of high stress soil behavior with the MIT-S1 constitutive model (Jaeger 2012). In addition, FLAC modelling has been used to model cone penetration in sands and clays (Moug et al 2019). The MIT-S1 constitutive model was implemented in FLAC with a user defined model via dynamic link library (dll) file. The MIT-S1 module used in this study is a modified version of the module used by Jaeger (2012) and validated in Moug et al. (2019). A detailed description of the MIT-S1 user defined model implementation in FLAC can be found in Jaeger (2012).

3.1 MIT-S1 Calibration Approach

In order to calibrate the MIT-S1 model in FLAC to the laboratory produced data, it was necessary to establish the material properties of the soil specimens being studied. As previously discussed, key parameters of the MIT-S1 model can be derived from LCC characterization of the soil under high stress 1-D compression, specifically ρ_c, $\sigma_{v,ref}$, and θ. These parameters are found through fitting a curve to the LCC data plotted in log-log e - stress space. Additionally, the parameter of C_b can be solved for explicitly using the following equations from Jaeger (2012):

$$\frac{K_{max}}{p_{atm}} = C_b\left(\frac{1}{e^{1.3}}\right)\left(1+\left(\frac{K_{max}}{2G_{max}}\right)\eta:\eta\right)^{\frac{n}{2}}\left(\frac{p'}{p_{atm}}\right)^{n} \qquad 3.1$$

$$\frac{G_{max}}{p_{atm}} = \frac{1}{2}C_b\left(\frac{1}{e^{1.3}}\right)\left(\frac{2G_{max}}{K_{max}}\right)\left(1+\left(\frac{K_{max}}{2G_{max}}\right)\eta:\eta\right)^{\frac{n}{2}}\left(\frac{p'}{p_{atm}}\right)^{n} \qquad 3.2$$

G_{max} and K_{max} can be found with the following equations:

$$G_{max} = \rho V_s^2 \qquad 3.3$$

$$K_{max} = \frac{2G_{max}(1+\upsilon)}{3-6\upsilon} \qquad 3.4$$

where ρ is density, V_s is shear wave velocity, υ is Poisson's ratio, p_{atm} is reference atmospheric pressure and e is void ratio. The term $\eta:\eta$ describes the position of the stress state relative to the yield surface in generalized, non-triaxial compression. Calculation of $\eta\colon\eta$ follows the format of

$$A\colon B = tr\left(A_{ij}B_{jk}\right) = A_{ij}B_{ij} \tag{3.5}$$

where *i*, *j*, and *k* are indices corresponding to spatial coordinates (Jaeger 2012). The $\eta\colon\eta$ calculation performed for this calibration assumed a K_0 of 0.5 and was calculated as follows:

$$\eta_{ij} = \frac{S_{ij}}{p'} \tag{3.6}$$

$$S_{ij} = \begin{bmatrix} \sigma'_{11} - p' & \sigma'_{12} & \sigma'_{13} \\ \sigma'_{21} & \sigma'_{22} - p' & \sigma'_{23} \\ \sigma'_{31} & \sigma'_{32} & \sigma'_{33} - p' \end{bmatrix} \tag{3.7}$$

The following equation represents $\eta\colon\eta$ for principle stress loading conditions in 1-D compression:

$$\eta\colon\eta = \left[\frac{\sigma'_1 - p'}{p'}\right]^2 + \left[\frac{\sigma'_2 - p'}{p'}\right]^2 + \left[\frac{\sigma'_3 - p'}{p'}\right]^2 \tag{3.8}$$

For a K_0 value of 0.5 and σ'_1 value of 200kPa, σ'_2 and σ'_3 are both 100kPa, p' is 133.3kPa and the final calculated value of $\eta\colon\eta$ is 0.375.

The remaining parameters for the MIT-S1 constitutive model were determined through the use of accepted values (Price 2018) and curve matching to lab data. The final parameter values and descriptions are listed in Table 3.1. Values for the parameters of $D_p, r_p, h_p, \omega, \omega_s$ and ψ were chosen as typical values for intermediate soils as shown in Price (2018). Values for the parameters of ϕ'_{cs}, $\phi'_{mr}, m_p, p_{\varphi}$, and μ_0 were chosen by comparison to lab data plots (Figures 3.3, 3.4, and 3.5) generated from soil specimens subjected to 1-D consolidation and undrained direct simple shear (UDSS) tests. Consolidation and UDSS lab tests for the specimens used in this calibration were performed by Melissa Preciado (Preciado 2021). The parameters were held to reasonable value ranges (see Section 3.3) and adjusted one at a time to observe the effect of the changes.

Calibration of the MIT-S1constitutive model for UDSS loading was performed using single element simulations in FLAC. Elements in the simulation were initialized at specific stresses and then unloaded to achieve the desired over consolidation ratio (OCR). Simulation specimen OCR values were chosen to match the OCR values of data produced from lab testing of soil specimens.

3.2 Calibration Results

Using the above described methods, the final calibration values for the MIT-S1 parameters of the Portland-area soil was determined. Values can be seen in Table 3.2. Further discussion of individual parameter results follows.

The initial requirements for calibrating the MIT-S1 model are the compression characteristics found using the high-stress pneumatic load frame described in Section 2.1. As previously discussed, subjecting the soil to high stresses in 1-D compression and plotting the resulting lab data in a log-log, *e* – vertical stress space allows us to curve fit the MIT-S1 parameters ρ_c and θ, and to calculate $\sigma'_{v,ref}$ which were found to be 0.53, 0.31, and 21.7 atm, respectively (Figure 3.2).

The 1-D compression was performed using a slurry mixture created from soil retrieved from the Sunderland site. A total of seven compression tests were performed with a single preparation of the slurry mixture. It should be noted that further refinements of the compression component of the calibration could be performed with different slurry mixture preparations of soils retrieved from different locations within the same soil unit. This was not possible for this research due to limitations imposed by the COVID-19 pandemic. However, the parameter values derived from the laboratory compression tests are generally comparable to those values found in previous research on similar soils (Price 2018) which lends confidence to the results being a reasonable representation of the soils compression behavior.

The remaining MIT-S1 parameters were derived from analysis of laboratory data of undrained direct simple shear tests performed on trimmed, undisturbed soil specimens or from previous research results of comparable soils (Price 2018) as described in Section 3.1. The noteworthy parameters for this calibration were for critical state friction angle (ϕ'_{cs}), reference friction angle (ϕ'_{mr}), bounding surface geometry (m) and contractive-dilative transition (p_{φ}). As previously discussed, these values were adjusted to calibrate the model results produced from FLAC to match lab data results. From the single element simulation results, the best fit values of ϕ'_{cs} and ϕ'_{mr} were found to be 34° and 36° while the best fit values of m and p_{φ} were found to be 0.9 and 0.7, respectively. Figures 3.3 and 3.4 show model results plotted with lab data.

When calibrating the model, it was necessary to prioritize certain characteristics over others. The lab data for undrained direct simple shear generally shows a much softer initial response while the model results were generally much stiffer. This was likely a result of using stiffness parameter values derived from shear wave velocity characteristics obtained from in-situ testing, in contrast to the softer response of laboratory-prepared specimens due to sample disturbance during sampling, transportation, and specimen preparation. The calibration of the constitutive model was intended for use with in-situ tests such as the CPT, therefore in-situ stiffness and peak shear stress values were prioritized over position of the peak stress relative to strain. The model results generally show peak shear stress at smaller strain values when compared to the lab data. Additionally, preference was given to calibrating the model to undrained shear strength normalized to vertical effective strength vs OCR (Figure 3.5).

The position of initial consolidation conditions created in the single element simulations was compared to the theoretical critical state line (CSL) as shown in Figure 3.6 to evaluate reasonable load path assumptions for the model calibration. The theoretical CSL was generated from the MIT-S1 input parameters that characterize shear behavior of soil. For this figure, the CSL is plotted for shear in triaxial compression using mean effective stress for the horizontal axis. The loading paths shown on Figure 3.6 are for UDSS loading, so the load paths do not necessarily intersect the triaxial compression CSL. However, it is reasonable to use as a guide as differences between UDSS and triaxial compression shearing are minimal in the context of this calibration.

As discussed in Pestana & Whittle (1999), clays and clay-like soils will produce a CSL that is parallel with the LCC in a log-log $e - p'$ space. In addition, sands will produce a CSL that is approximately parallel to the LCC in a log e -log p' space under high stresses. Using the shear behavior parameter values that were estimated through simulated UDSS tests, the CSL produced for this calibration becomes approximately parallel only at higher stress values. However, the stress values where the CSL approaches parallel with the LCC are lower than typical values of sands, implying an intermediate soil.

3.3 Calibration Discussion

Calibrating a constitutive model to specific soil behaviors presents a number of challenges. Of paramount concern is ensuring that the model is representative of realistic soil characteristics and avoiding arbitrary parameter values which are unreasonable. It is possible to create a model which outputs figures that match well with lab data but contain values which are not likely to be represented in reality. Care was taken to evaluate the reasoning behind choosing the final calibration values. This section will discuss the sensitivity of the model to the different parameters under consideration as well as other issues that were addressed during the course of the research project.

Data generated from lab results generally has a softer initial response during direct simple shear than the equivalent numerical model. Therefore, priority in plot matching was given to peak and critical state shear stress response rather than initial elasto-plastic response. This results in a leftward shift in peak shear stress versus shear strain when compared to lab results (Figure 3.3). In addition, the lab data shows variation in vertical effective stress through the initial shearing phase prior to reaching peak shear stress for OCR's 2 and 4, with OCR 2 indicating compressive behavior and OCR 4 indicating dilative behavior. In contrast, the model indicates no change in vertical effective stress until after reaching peak shear stress values (Figure 3.4). Lab data and model results largely conform to one another for the normally consolidated case.

It was not feasible given time constraints and the scope of this project to attempt a calibration that was inclusive of soil-specific adjustments to all of the MIT-S1 parameters. Priority was given to those parameters which show significant sensitivity for intermediate soils, specifically friction angle (ϕ'_{cs} and ϕ'_{mr}), bounding surface geometry (m), and contractive-dilative transition (p_{φ}). These four parameters describe the shear behavior of the soil in the MIT-S1 constitutive model as well as influencing the size and shape of the yield surface boundary. These parameters also have an impact on the shape and position of the critical state line in a semi-log e – p'_{cs} (or σ'_{v}) space. More detailed discussion of the individual parameters and their effect on the model calibration follows.

Critical state friction angle, ϕ'_{cs}, is a parameter that is used widely in the field of geotechnical engineering. The parameter describes the friction angle of granular or intermediate soils when volume change during shearing is at or near zero. Figure 3.7 shows the sensitivity to the MIT-S1 model to different values of ϕ'_{cs}. For normally consolidated specimens, the sensitivity of the loading path to critical state conditions is low. As OCR increases, the effect of ϕ'_{cs} is also increased. A shift from contractive to dilative behavior is evident in elements consolidated to OCRs 2 and 4 when ϕ'_{cs} is reduced and the converse is true when ϕ'_{cs} is increased. Additionally, an increase in peak shear stress is evident when ϕ'_{cs} values are reduced and a reduction in peak shear stress is observed when ϕ'_{cs} is increased. These changes in peak shear stress for OCR = 2 and OCR = 4 are related to the construction of the MIT-S1 constitutive model yield surface, where the yield surface shape and size are not affected by changes in ϕ'_{cs}.

The reference maximum friction angle, ϕ'_{mr}, is a parameter related to maximum friction angle (ϕ'_m), where $\phi'_{mr} = \phi'_m$ at $e = 1$. Maximum friction angle is a density dependent parameter in which ϕ'_m approaches $45 + \phi'_{cs}/2$ as e approaches zero (Pestana and Whittle 1999). The MIT-S1 model shows a similar, albeit somewhat more significant, sensitivity to ϕ'_{mr} as it does to ϕ'_{cs} (Figure 3.8). ϕ'_{mr} is related to both the size of the yield surface, and the position of the CSL. As ϕ'_{mr} increases, the yield surface size increases and the CSL shifts to higher stress conditions. Therefore, changes in soil behavior with changes in ϕ'_{mr} reflect both of these changes. The model is more reactive to variations in this parameter at higher OCR's and the change in contractive versus dilative behavior is evident. The degree of these variations is more pronounced than with ϕ'_{cs}.

The parameter of m influences the size and shape of the yield surface boundary in a normalized shear stress – mean effective stress space (Figure 3.9). As m increases the size of the yield surface increases. This has an effect on elasto-plastic deformations of the soil in shear. In granular and intermediate soils, m influences the transition from contractive to dilative behavior (Pestana and Whittle 1999). With this parameter, a reduced value is associated with contractive behavior and an increased value with dilative behavior (Figure 3.10). The model shows more sensitivity to this parameter on normally consolidated soils, as opposed to the friction angle parameters.

The final parameter under consideration for this calibration is p_{φ}, which is a friction angle dependent parameter which contributes to contractive-dilative behavior. The parameter p_{φ} relates the parameter ϕ'_{mr} to ϕ'_{m} (Pestana and Whittle 1999). A larger p_{φ} value results in a ϕ'_{m} parameter that is more sensitive to changes in e, whereas for $p_{\varphi} = 0$ there is no change in ϕ'_{m} with e. A p_{φ} of 0 indicates a clay or clay-like soil, while a $p_{\varphi} > 0$ indicates a sand, sand-like, or intermediate soil (Jaeger 2012). Setting the parameter to zero in the model simulation resulted in errors as the load paths for some elements would not approach the CSL. This served as a confirmation that the model was representative of an intermediate type soil. Model sensitivity to p_{φ} is not as significant as it was to the parameters of ϕ'_{cs}, ϕ'_{mr}, and m and model variation with different values was relatively low (Figure 3.11). However, it was a necessary component in defining the CSL, which was a primary concern when including it as one of the major components of the calibration.

3.4 Figures

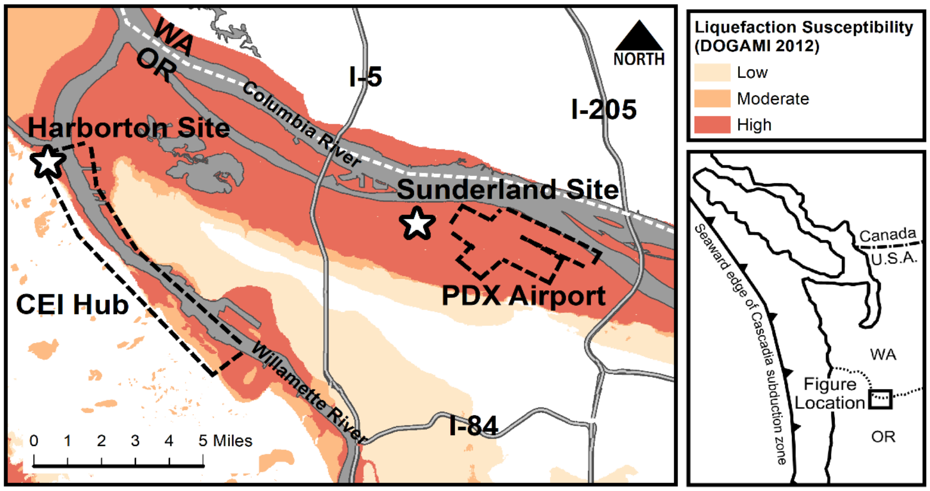

Figure 3.1: Map showing the location of the Sunderland site where soil specimens used for LCC characterization were sourced (reprinted from Sorenson 2020)

Table 3.1: General soil properties from Sunderland research site (reproduced from Preciado et al 2021)

Depth range below ground surface	Water content (%)	Void ratio	Atterberg Limits	Gradation	In situ OCR	Estimated in situ vertical effective stress (kPa)	CPT, qc (kPa)	I_c[e]	V_s[f] (m/s)	V_p[f] (m/s)
1.2 m – 2.0 m	34-45	1.06-1.24	LL= 38% PL= 25% PI= 13[a] (5)[b]	Sand = 10% Silt = 70% Clay = 20%	4[c]	26	450	3.0	80-100	600-1000
4.3 m – 5.3 m	40-59	1.23-1.32	LL= 48% PL= 31% PI= 17[a] (6)[b]	Sand = 5% Silt = 75% Clay = 20%	2.3[d]	48	480	2.8	95-110	1450 - 1675

[a] average value, [b] standard deviation, [c] estimated from CPT correlations, [d] measured from consolidation test, [e] based on Robertson (2009), [f] based on DPCH and crosshole measurements

Table 3.2: Material Properties Table for MIT-S1 Calibration

Parameter	Description	Value
K_{0NC}	Coefficient of lateral earth pressure	0.49
ρ_c	Slope of limiting compression curve (LCC)	0.53
θ_p	Transitional compression behavior	0.31
$\sigma'_{v,ref}$	Reference vertical effective stress	21.7
D_p	Non-linear volumetric swelling and hysteresis	0.04
r_p	Non-linear volumetric swelling and hysteresis	0.45
h_p	Irrecoverable plastic strain	6.0
C_b	Small strain stiffness at load reversal	475
μ_0	Poisson's ratio at stress reversal	0.25
ω	Non-linear Poisson's ratio	1.0
ω_s	Small strain non-linearity in shear	8.0
φ'_{cs}	Critical state friction angle	34.0
φ'_{mr}	Maximum friction angle of bounding surface at void ratio of 1.0	36.0
p_φ	Transition from contractive to dilative behavior	0.5
m	Geometry of bounding surface	0.9
ψ	Rotation of bounding surface	60.0

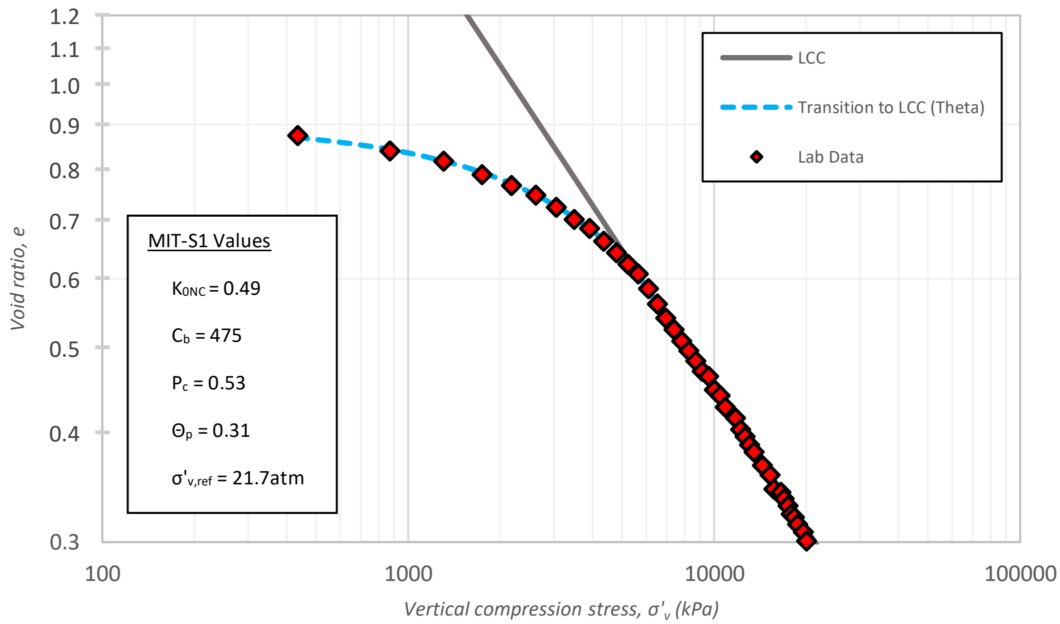

Figure 3.2: 1-D compression plot for Sunderland soil slurry mixture showing LCC and compression path transition, θ

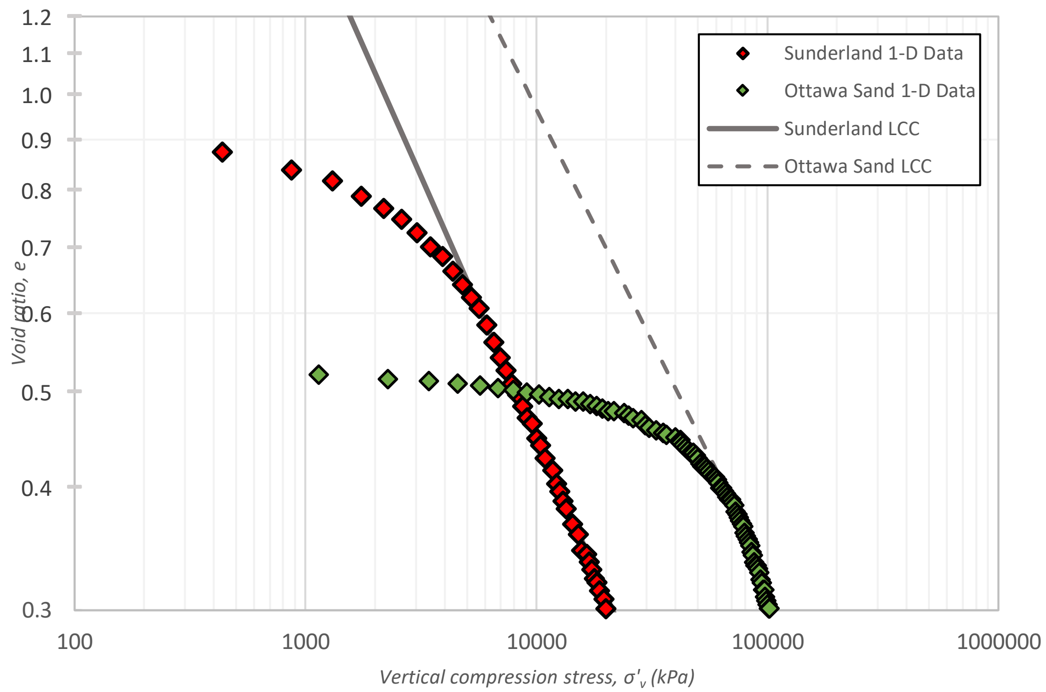

Figure 3.3: 1-D compression plot comparison for Sunderland soil slurry mixture and Ottawa sand showing LCC

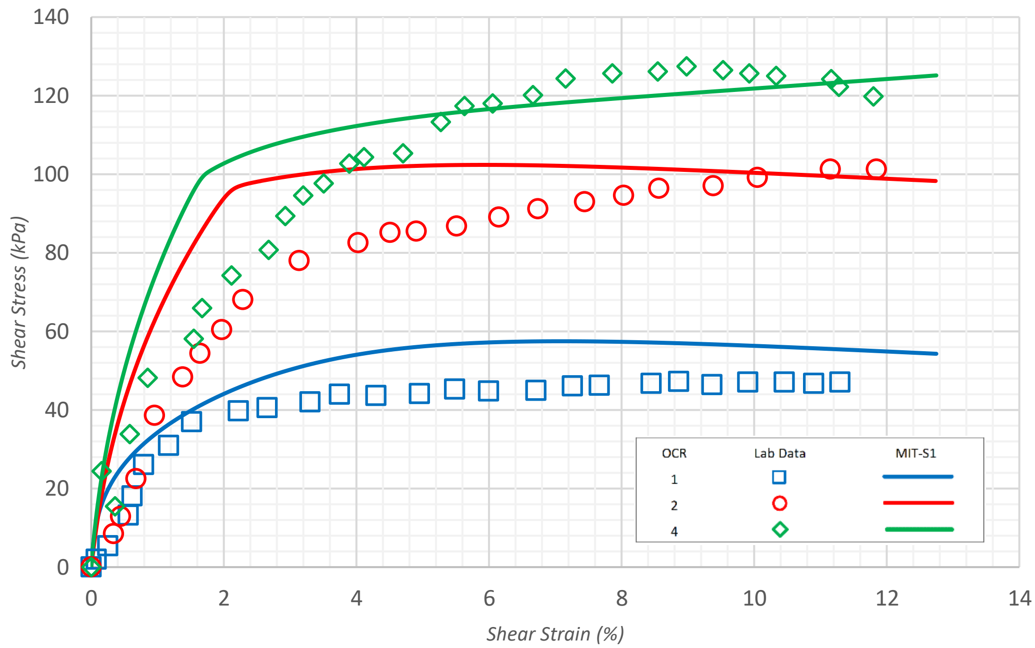

Figure 3.4: Shear stress vs shear strain comparison of Sunderland soil specimen in undrained direct simple shear and representative MIT-S1 model results

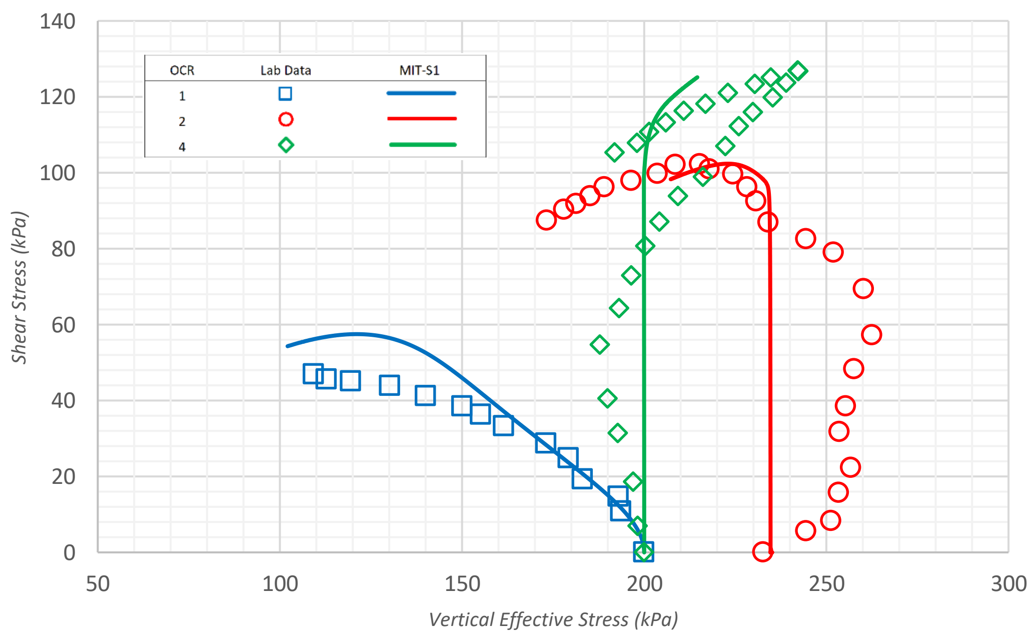

Figure 3.5: Shear stress vs vertical effective stress comparison of Sunderland soil specimen in undrained direct simple shear and representative MIT-S1 model results

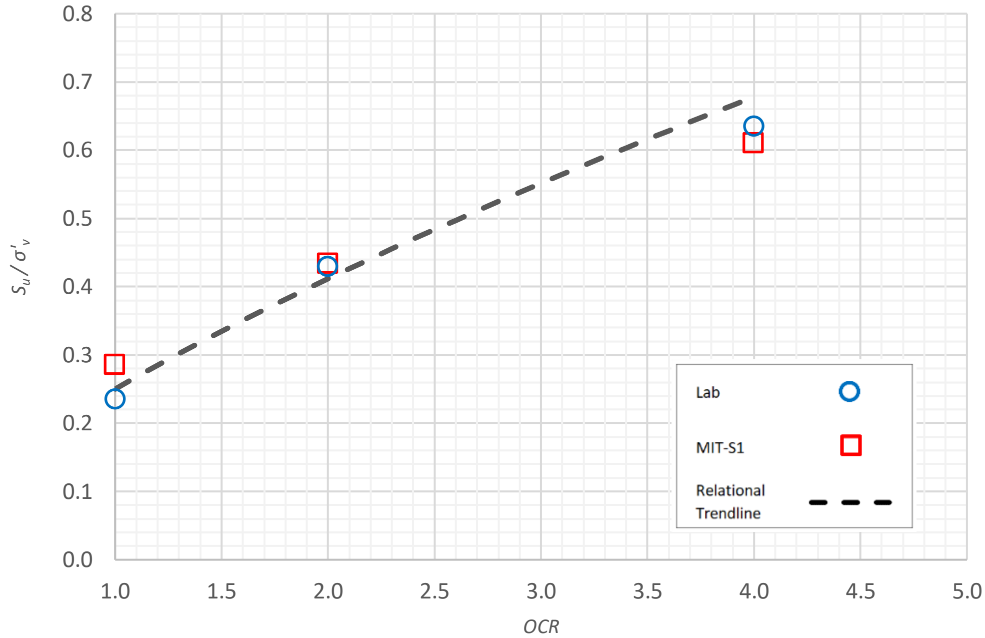

Figure 3.6: Normalized relationship curves (S_u / σ'_v) for direct simple shear comparing simulated MIT-S1 model properties and lab data.

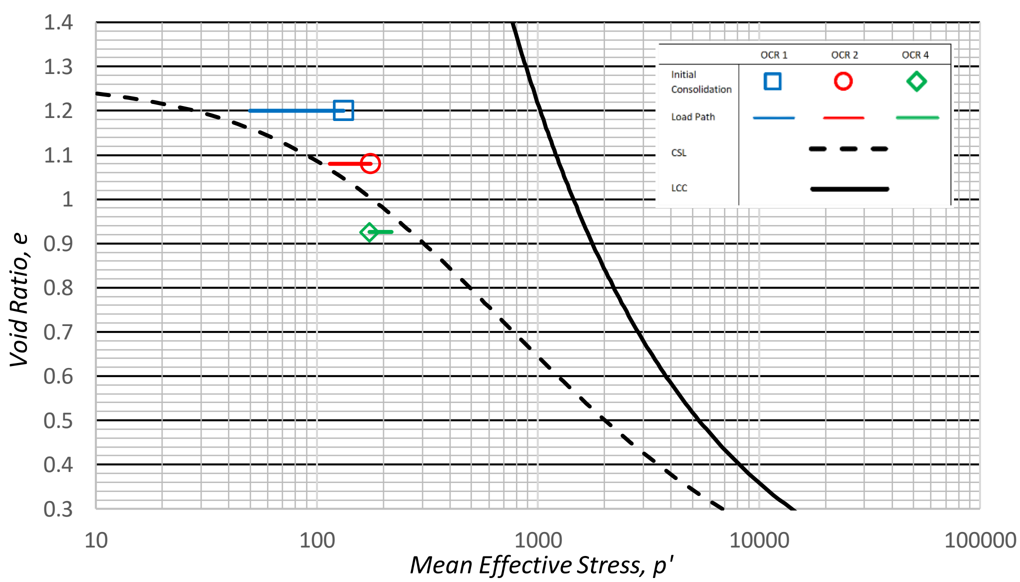

Figure 3.7: Triaxial compression Critical State Line (CSL) and Limiting Compression Curve (LCC) plotted with simulated single element initial soil consolidation states and respective load paths.

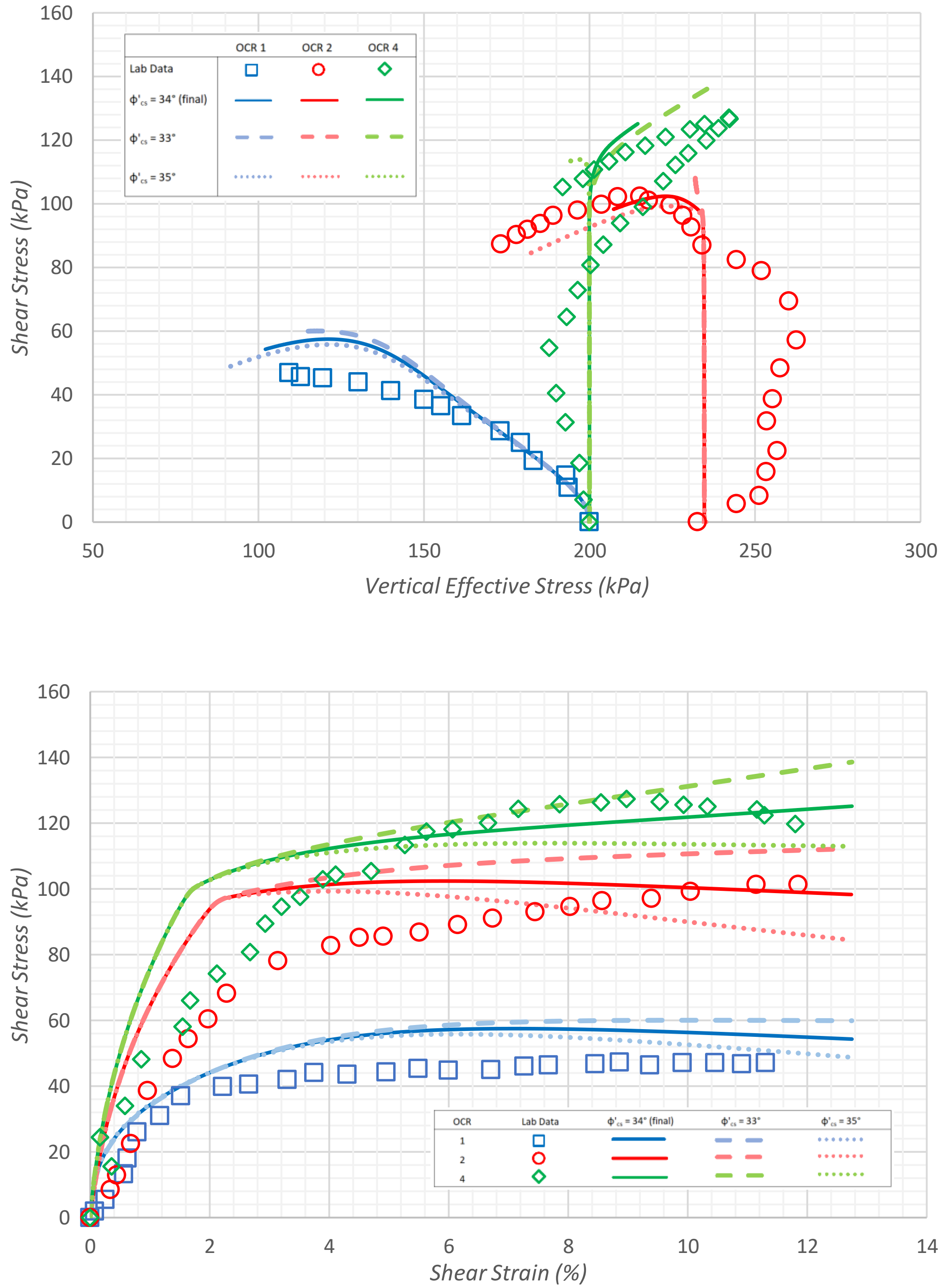

Figure 3.8 (a) and (b): Comparison plot showing bracketed model results for ϕ'_{cs} values of 33°, 34°, and 35°. All other MIT-S1 parameters are retained.

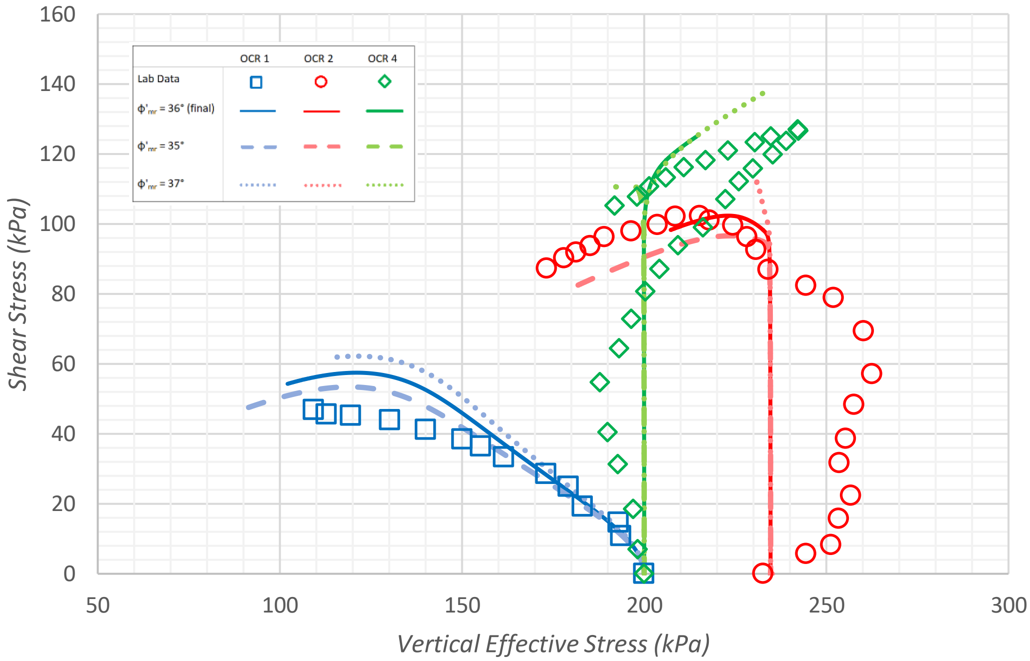

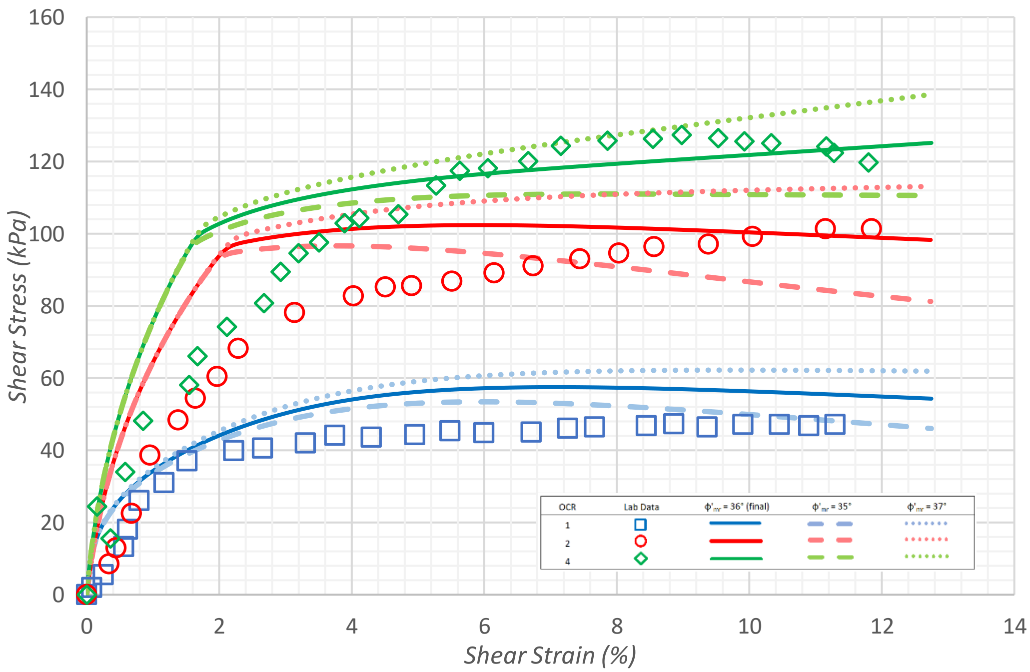

Figure 3.9 (a) and (b): Comparison plot showing bracketed model results for ϕ'_{mr} values of 35°, 36°, and 37°. All other MIT-S1 parameters are retained.

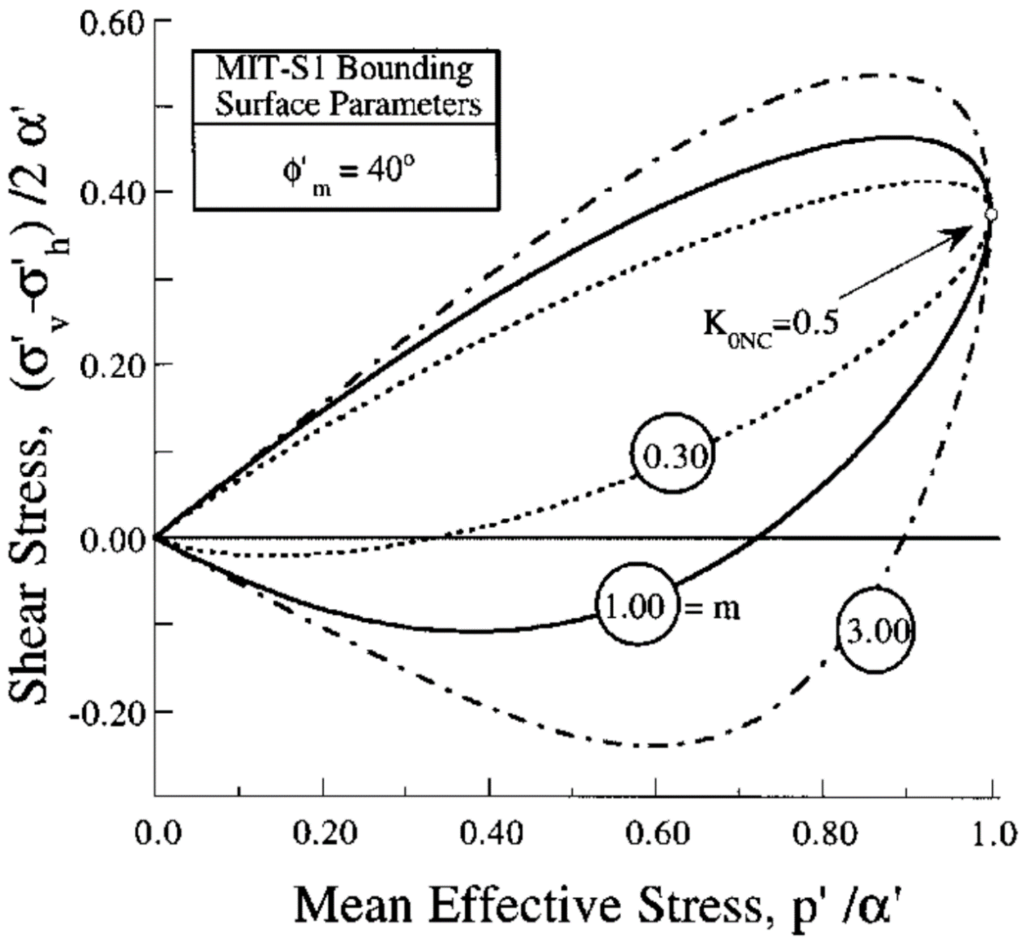

Figure 3.10: Effect of MIT-S1 parameter *m* on boundary surface geometry in normalized shear stress - mean effective stress space (reproduced from Pestana & Whittle 1999)

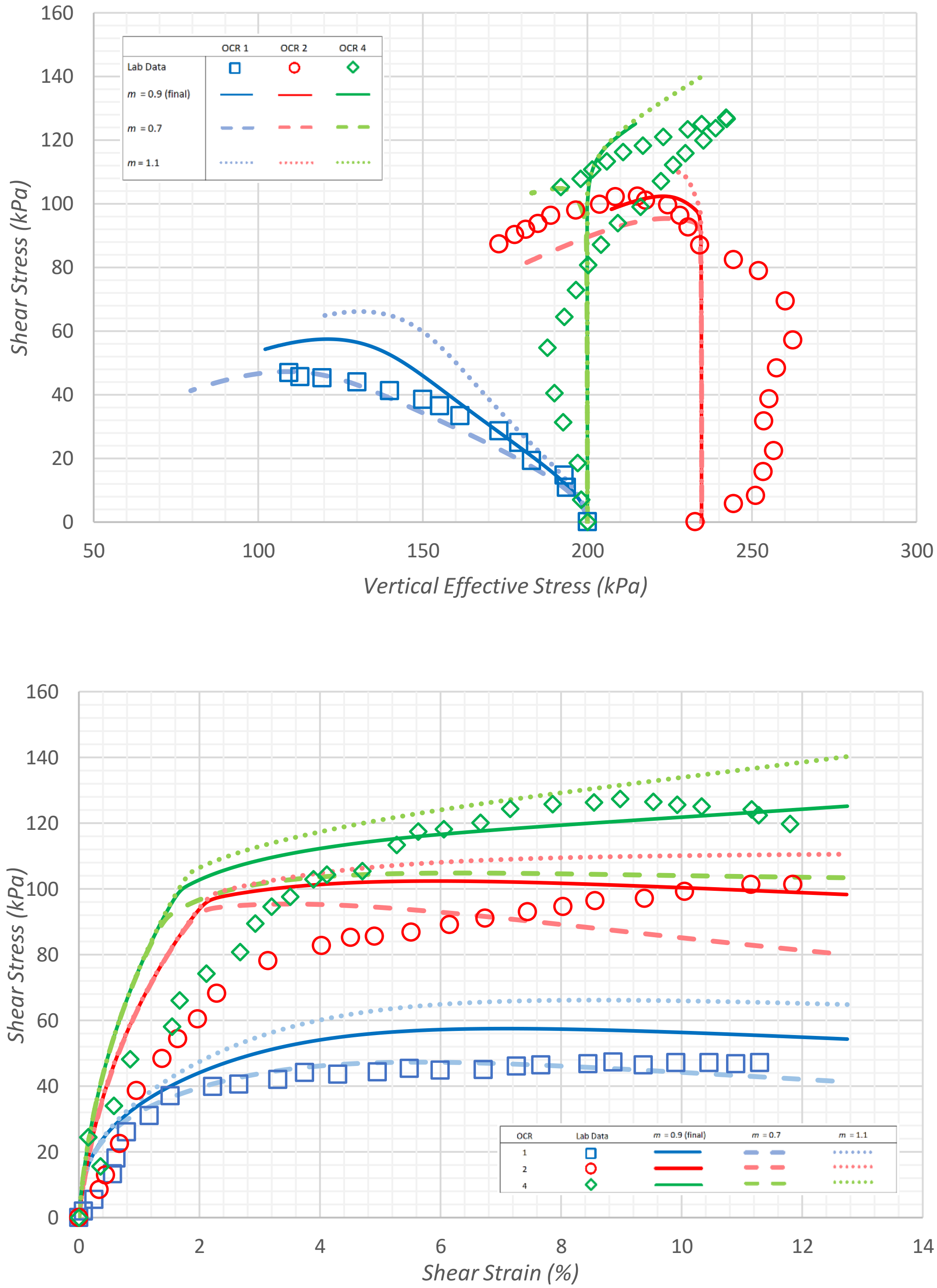

Figure 3.11 (a) and (b): Comparison plot showing bracketed model results for m values of 0.7, 0.9, and 1.1. All other MIT-S1 parameters are retained.

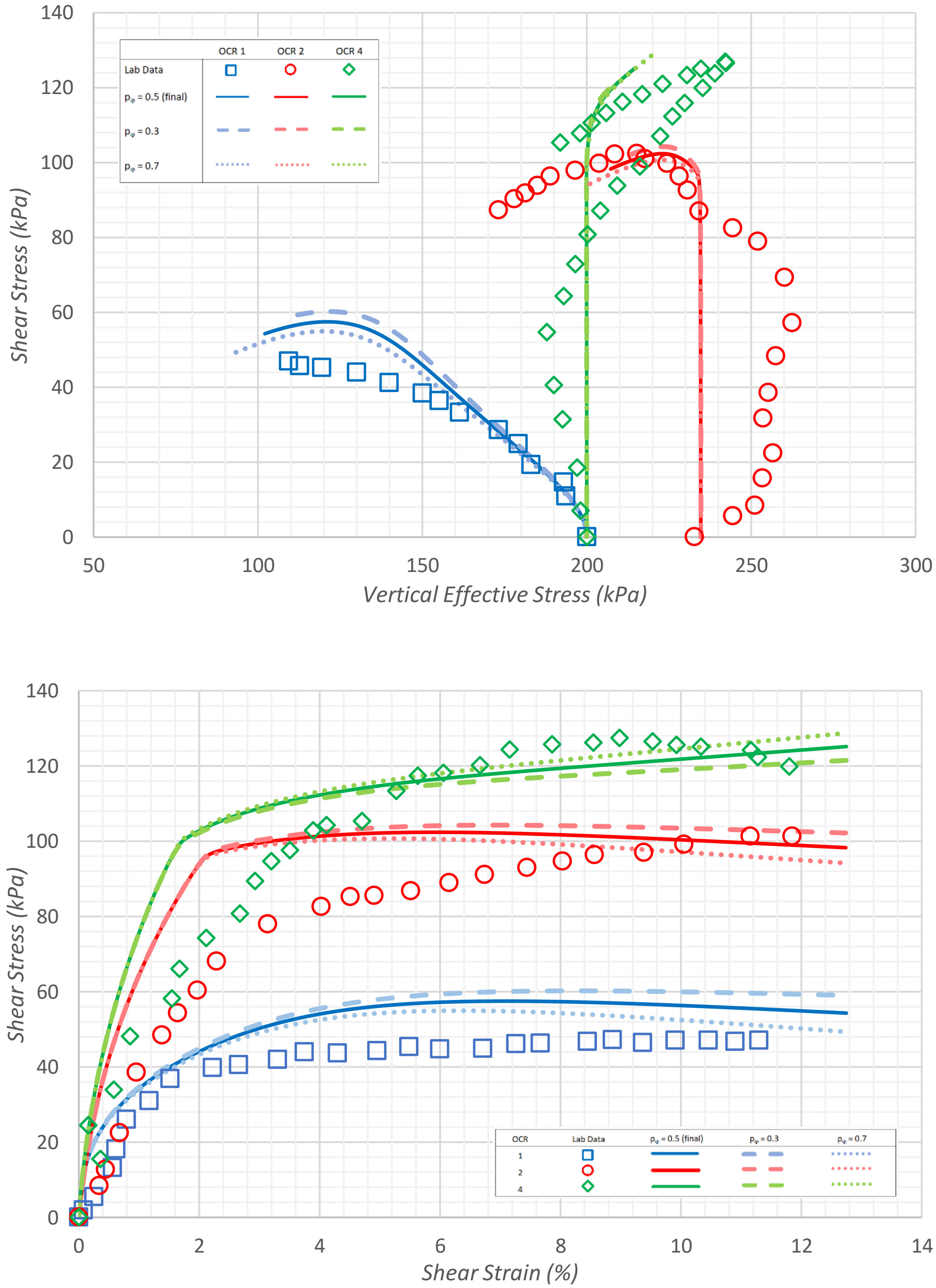

Figure 3.12 (a) and (b): Comparison plot showing bracketed model results for p_{φ} values of 0.3, 0.5, and 0.7. All other MIT-S1 parameters are retained.

4. Conclusions

This goal of this research was to develop an MIT-S1 calibration for a Portland-area intermediate soil. MIT-S1 parameters were calibrated with (i) 1-D compression tests to high stresses to determine the parameter values for the Limiting Compression Curve, (ii) undrained direct simple shear tests to calibrate shear behavior, and (iii) parameters guidance based on values from previous research and calibrations on similar soils. Care was taken to preserve reasonable parameter values relative to understood theoretical practices, such as critical state mechanics.

This project involved verifying and performing suitable 1-D compression testing procedures for the lab at PSU, for the purpose of characterizing the limiting compression curve of silt slurry mixtures created from a locally sourced soil sample. In order to perform the 1-D compression testing, it was necessary to have a specimen mold and piston device custom designed and built. The testing procedure and mold were validated with compression testing on Ottawa F-65 sand. 1-D compression testing was also performed on a slurry-prepared specimen of a low plasticity (ML type) Portland-area intermediate soil with a plasticity index of approximately 15 and a fines content of approximately 95%.

Shear behavior of the soil was calibrated from UDSS tests on intact specimens. The tests were performed for approximate OCRs of 1, 2, and 4. The shear calibration was done using single element simulations using finite difference modeling software FLAC and the output from the simulations was compared to laboratory UDSS tests. In addition, the simulation results were compared with expected behaviors from critical state theory to determine dilative and contractive behavior during shear to further verify that the model calibration represented reasonable soil characteristics. In addition, the relationship of the CSL to the LCC was shown to become approximately parallel under relatively high stress. This implies that the soil is not a clay or a clay-like. The stress values at which the CSL approaches a parallel relationship with the LCC are lower than typical values for pure sands, implying the calibration of an intermediate soil with the finalized parameter values.

By combining the values estimated from high-stress 1-D compression tests and UDSS tests performed in the laboratory and the values determined from single element UDSS simulations, a reasonable calibration of the MIT-S1 constitutive model for a Portland-area intermediate soil was achieved. Following this work, the next steps will be to simulate cone penetration with this constitutive model calibration to examine cone penetration test data in an intermediate Portland-area soil.

References

Boulanger, R. W., and Idriss, I. M., (2016). "CPT-based liquefaction triggering procedure". *J. Geotech. Geoenviron. Eng.*, 142 (2)

Jaeger, R. A. (2012). "Numerical and experimental study on cone penetration in sands and intermediate soils". PhD thesis, Dept. of Civil and Environmental Engineering, Univ. of California, Davis.

Moug, D. M., Boulanger, R. W., DeJong, J. T., Jaeger, R. A., (2019). "Axisymmetric simulations of cone penetration in saturated clay". *J. Geotech. Geoenviron. Eng.*, 145(4)

Parra Bastidas, A. (2016). "Ottawa F-65 sand characterization". PhD thesis, Dept. of Civil and Environmental Engineering, Univ. of California, Davis.

Pestana, J., and Whittle, A. (1995). "Compression model for cohesionless soils". *Géotechnique*, 45(4), 611-631.

Pestana, J., and Whittle, A. (1999). "Formulation of a unified constitutive model for clays and sands". *Int. J. Numer. Anal. Meth. Geomech.*, 23 (12), 1215-1243.

Pestana, J., Whittle, A., and Gens, A. (2002). "Evaluation of a constitutive model for clays and sands, Part II: Clay behavior". *Int. J. Numer. Anal. Meth. Geomech.*, 26 (11), 1123-1146.

Preciado, A. M., Sorenson, K., Khosravifar, A., Moug, D., Stokoe, K., Menq, F., Zhang, B., (2021, forthcoming). “Evaluating cyclic loading response of a low plasticity silt with laboratory and field cyclic loading tests”. *ASCE Lifelines 2021 Conference UCLA*

Price, A. B. (2018). "Cyclic strength and cone penetration resistance for mixtures of silica silt and kaolin". PhD thesis, Dept. of Civil and Environmental Engineering, Univ. of California, Davis.

Sorenson, K., Preciado, A. M., Moug, D., Khosravifar, A., van Paasen, L., Kavazanjian, E., Stokoe, K., Menq, F., (2021, forthcoming). "Field monitoring of the persistence of desaturation for mitigation of earthquake induced soil liquefaction in silty soil". *ASCE Lifelines 2021 Conference UCLA*